

Chronic hyponatremia exacerbates multiple manifestations of senescence in male rats

Julia Barsony · Michaele B. Manigrasso · Qin Xu · Helen Tam · Joseph G. Verbalis

Received: 26 July 2011 / Accepted: 23 November 2011 / Published online: 5 January 2012
© American Aging Association 2011

Abstract The syndrome of inappropriate antidiuretic hormone secretion (SIADH) is frequently responsible for chronic hyponatremia in the elderly due to age-related disruption of the inhibitory component of brain osmoregulatory mechanisms. Recent research has indicated that chronic hyponatremia is associated with gait disturbances, increased falls, and bone fragility in humans, and we have found that chronic hyponatremia causes increased bone resorption and reduced bone mineral density in young rats. In this study, we used a model of SIADH to study multi-organ consequences of chronic hyponatremia in aged rats. Sustained hyponatremia for 18 weeks caused progressive reduction of bone mineral density by DXA and decreased bone ash calcium, phosphate and sodium contents at the tibia and lumbar vertebrae. Administration of 10-fold higher vitamin D during the last 8 weeks of the study compensated for the reduction in bone formation and halted bone loss. Hyponatremic rats developed hypogonadism, as indicated by slightly lower serum testosterone and higher serum FSH and LH concentrations, markedly decreased testicular weight, and abnormal testicular

histology. Aged hyponatremic rats also manifested decreased body fat, skeletal muscle sarcopenia by densitometry, and cardiomyopathy manifested as increased heart weight and perivascular and interstitial fibrosis by histology. These findings are consistent with recent results in cultured osteoclastic cells, indicating that low extracellular sodium concentrations increased oxidative stress, thereby potentially exacerbating multiple manifestations of senescence. Future prospective studies in patients with SIADH may indicate whether these multi-organ age-related comorbidities may potentially contribute to the observed increased incidence of fractures and mortality in this population.

Keywords Aged rats · Cardiomyopathy · Hypogonadism · Hyponatremia · Osteoporosis · Sarcopenia · Syndrome of inappropriate antidiuretic hormone secretion

Introduction

Chronic hyponatremia, defined as a serum sodium ion concentration ($[Na^+]$) <135 mmol/l, is the most common electrolyte disorder encountered in clinical practice, and is especially common in the elderly. The prevalence of hyponatremia was estimated in the range of 3.2–6.1 million persons in the U.S. annually; 75–80% of hyponatremia was chronic and asymptomatic, 13–20% were treated in an outpatient setting, and the prevalence of hyponatremia increased progressively

J. Barsony (✉) · M. B. Manigrasso · Q. Xu · H. Tam · J. G. Verbalis (✉)
Division of Endocrinology and Metabolism,
Georgetown University,
Washington, DC 20007, USA
e-mail: jb394@georgetown.edu
e-mail: verbalis@georgetown.edu

with increasing age (Boscoe et al. 2006; Hawkins 2003). Until recently, no effective and tolerable treatment was available for chronic hyponatremia. The recent FDA approval of the oral medication, tolvaptan, which effectively corrects hyponatremia by antagonizing vasopressin V2 receptors in the kidney collecting duct, offers the possibility to reverse chronic hyponatremia (Greenberg and Verbalis 2006). Consequently, studies aimed at understanding the long-term adverse effects of hyponatremia are both timely and important for public health.

Adaptation to the external environment requires maintenance of water and sodium balance within relatively narrow ranges. Ageing weakens the ability of individuals to respond to environmental challenges, which explains why chronic hyponatremia is frequently found in geriatric patients. Although chronic hyponatremia is frequently considered to be asymptomatic, recent reports indicate that chronic hyponatremia presents a significant health problem in the elderly population, leading to subtle but life-changing consequences including attention deficits (Miyazaki et al. 2010), increased fall risk (Renneboog et al. 2006), osteoporosis and fractures (Kinsella et al. 2010; Verbalis et al. 2010), and increased mortality of both inpatients (Wald et al. 2010) and outpatients (Hoorn et al. 2011).

Although about one third of the body sodium is stored in bone (Bergstrom and Wallace 1954), surprisingly little is known about the consequences of sodium balance abnormalities on bone. We have recently reported that chronic hyponatremia was associated with low bone mineral density (BMD) in rat model of the syndrome on inappropriate antidiuretic hormone secretion (SIADH) (Verbalis et al. 2010). Pronounced hyponatremia for 3 months in these young adult rats was well tolerated, but resulted in severe osteoporosis (decrease of BMD was 30% by densitometry, 80% by microcomputed tomography, and 60% by bone histomorphometry). The young hyponatremic rats had lower serum 25-hydroxy-vitamin D (25OHD) and 1, 25-dihydroxvitamin D levels and mild hypogonadism (slightly lower serum testosterone and higher FSH) than normonatremic rats, but these abnormalities could not fully explain the observed bone loss. However, histomorphometry demonstrated markedly increased numbers of osteoclasts associated with trabecular surfaces in sections from the femora and vertebrae of hyponatremic rats compared to controls, and dynamic histomorphometry also indicated decreased bone formation.

Additional studies of the mechanisms responsible for hyponatremia-induced bone loss and osteoporosis were done *in vitro* in RAW264.7 murine pre-osteoclastic cells, and showed that hyponatremia directly activates osteoclastogenesis and osteoclastic bone resorption (Barsony et al. 2010). Furthermore, a sodium concentration dependent decrease in the activity of the sodium-dependent vitamin C transporter, resulting in decreased ascorbic acid uptake, was found. Ascorbic acid is essential for osteoblast functions, including osteocalcin secretion (Wu et al. 2003) and is a negative regulator of osteoclastogenesis (Xiao et al. 2005). The decreased intracellular ascorbic acid concentration weakened the cellular defense against oxidative stress, increased the accumulation of free reactive oxygen radicals, and elicited multiple oxidative stress responses in these cells (Barsony et al. 2010).

Because oxidative stress is a well recognized mediator of aging-related multi-organ pathologies (Sohal and Weindruch 1996), in these studies we explored the effects of chronic hyponatremia on aging bone, including the time-course of bone loss, the significance of vitamin D and bone formation abnormalities, and the analysis of bone sodium and calcium content by ashing, and also the possibility that hyponatremia may have similar age-associated effects beyond bone. Senescence-associated chronic disorders have been described extensively and include senile osteoporosis characterized by low bone mass (Manolagas and Parfitt 2010), sarcopenia (Almeida et al. 2007; Frisoli et al. 2010), cardiac fibrosis (Wang et al. 2010), and hypogonadism (Sampson et al. 2007). We therefore studied the effects of chronic hyponatremia on bone, testes, and skeletal and cardiac muscle using a rat model of aging (Fisher 344 Brown-Norway F1; F344BN rats) to better approximate the elderly patient population most affected by chronic hyponatremia. These studies tested the hypothesis that chronically lowering the extracellular sodium concentration would exacerbate multiple manifestations of senescence due to increased oxidative stress (Barsony et al. 2010).

Methods

Animals and experimental design

All experimental procedures were performed according to the Guidelines for the Care and Use of Animals

available at the National Academies Press web site. The Institutional Animal Care and Use Committee of Georgetown University approved all animal experimentation according to federal and institutional policies and regulations. We used Fisher 344 Brown Norway F1 hybrid rats (F344BN; National Institute of Aging, supplied by Harlan–Sprague–Dawley, Indianapolis, IN). These rats have been extensively used for aging studies due to the lower incidence of chronic nephropathy compared to other inbred rat strains (Wahr et al. 2000). This aging rat model was also selected because after 26 months of age they demonstrate mild age-related osteoporosis (Perrien et al. 2007), decrease in lean body mass (Carter et al. 2010), cardiomyopathy (Capasso et al. 1990; Wahr et al. 2000), and androgen deficiency (Wang et al. 1993), resembling similar aging manifestations that occur in humans (Buford et al. 2010; Simon 1984; Swynghedauw et al. 1995). 22-month-old F344BN male rats (weighting 501.7 ± 31.6 g) were divided into two diet groups (solid and liquid) and acclimated to these diets for 2 weeks with close monitoring of baseline parameters. All rats were subsequently infused with the vasopressin V2 receptor agonist desmopressin (dDAVP; Aventis, Bridgewater, NJ) via subcutaneously implanted osmotic minipumps (Alzet Model 2004; Durect Co., Cupertino, CA) releasing dDAVP at a rate of $0.25 \mu\text{l/h}$ (5 ng/h). The pumps were replaced monthly to maintain continuous antidiuresis. This infusion of dDAVP alone does not produce hyponatremia in the absence of water loading. To produce hyponatremia, 15 animals were fed liquid diet (F5400sp; Bio-Serv) with a caloric density of 1.6 kcal/ml ($72 \text{ kcal day}^{-1} \text{ rat}^{-1}$), vitamin D₃ content of 3.2 IU/ml ($144 \text{ IU day}^{-1} \text{ rat}^{-1}$), and calcium content of 2 mg/ml ($90 \text{ mg day}^{-1} \text{ rat}^{-1}$). The normonatremic animals ($n=10$) received 15 g/day of solid diet (F5399; Bio-Serve) with a caloric density of 3.6 kcal/g ($54 \text{ kcal day}^{-1} \text{ rat}^{-1}$), vitamin D₃ content of 5 IU/g ($75 \text{ IU day}^{-1} \text{ rat}^{-1}$), and calcium content of 5.2 mg/g ($78 \text{ mg day}^{-1} \text{ rat}^{-1}$). Phase I of the study lasted for 10 weeks. During the Phase II of the study that lasted for an additional 8 weeks, hyponatremic animals received biweekly injections of vitamin D₃ ($70,000 \text{ IU/kg}$). At the end of the experiment, after dual energy X-ray absorptiometry (DXA) measurement and blood collection under inhalational anesthesia with isoflurane (3% in oxygen at 0.5 l/min), the isoflurane dose was increased until the lack of heart contraction and respiration indicated death.

Assessment of BMD and appendicular muscle mass by DXA

In vivo DXA measurements were taken under inhalation anesthesia with isoflurane using a small animal DXA scanner equipped with high-resolution scanning software, version 2.10 (Piximus, Lunar; GE, Madison WI). Two baseline measurements 1 week apart before pump implantation were followed by biweekly measurements performed nine times. BMD values were determined over the following areas: posterior–anterior (PA) view of the lumbar spine, lateral view of the lumbar spine (L1–L4), total femur, distal femur, and proximal tibia. Appendicular lean body mass was measured using the AP view images, within the area encompassing the left thigh muscle. Subcutaneous and visceral fat content changes were monitored using the lateral view images of the abdomen. The regions of interest were identical for the entire period, and the same size for every rat. Additionally, we assessed body composition within the lower left quarters of rats that fit into the imaging window of our densitometer: we recorded percent bone mineral content (BMC), lean and fat mass. At the end of the experiment, femora were excised, cleaned of soft tissue, and ex vivo BMD values were measured using the same Piximus scanner as described earlier (Verbalis et al. 2010).

Assessment of bone mineral content by ashing

BMC, wet weight, dry weight, and ash weight were recorded from both excised tibiae and combined L1–L2 vertebrae. After trimming of soft tissue and measurement of wet weight, bones were dried at 105°C for 48 h, dry weight measured, and then bones were placed into ceramic crucibles and incinerated at 700°C for 48 h in a furnace. Ash weights were recorded and ash contents were dissolved into 20 ml of 10% HNO_3 , and calcium, phosphorus, and sodium contents were determined with colorimetric assays (AniLytics Inc., Rockville, MD).

Testes and heart histology and morphometry

Testes were collected and weighed during autopsy, then preserved in 4% paraformaldehyde in PBS (pH 7.4), and stored at 4°C . Three testes from each group were randomly selected, dehydrated and embedded in

paraffin, and two sections from each block (5 μm thick) were stained with hematoxylin–eosin (H&E) and Masson's trichrome formulations. Additional sections were subjected to immunostaining using primary antibody against type I collagen (rabbit polyclonal; Abcam, San Francisco, CA) and horseradish peroxidase-labeled secondary antibody.

Hearts were collected at autopsy immediately after heart contractions stopped, trimmed of large vessels, weighed, then preserved in 4% paraformaldehyde in PBS (pH 7.4), and stored at 4°C. Five randomly selected hearts from each group were processed for histology: they were cut longitudinally across the great vessels to include the right and the left ventricles and septum in both parts, and the atria were trimmed. The remaining half parts were embedded into paraffin and 5- μm transverse sections were cut starting from the proximal end. Two sections (50 μm apart) from each heart were stained using H&E and another two using Masson's trichrome formulations.

We carried out all morphometric analysis using a Zeiss 410 inverted microscope fitted with a motorized stage and a Sony color camera, driven by software (Osteo II) from BioQuant Image Analysis Corporation (Nashville, TN). From testis samples, seminiferous tubule diameters along the short axis, and fractional area of blue stained collagen deposits per tubule area were determined. From both testes and heart samples, perivascular fibrosis (collagen) was quantified from 12 fields of view containing one arteriole (lumen diameter <100 μm), using a 20 \times objective, and expressed as fractional area determined by automatic color segmentation. The nature of the blue stained collagen deposit was confirmed by birefringence under polarized light and immunostaining for type I collagen (not shown). From the heart samples, fractional area of blue stained collagen between cardiac myocyte within 15,000 μm^2 total area were determined as interstitial collagen. Cardiac myocyte nuclei were counted within an 8,000- μm^2 area. Cardiac myocyte positioned perpendicularly to the plane of the section with a visible nucleus and cell membrane clearly outlined and unbroken were selected for the cross-sectional diameter measurements. Diameter measurements from 50 cells in each section were also collected automatically using a 40 \times objective and the inter-label distance tool (interval set to 5 μm) of the Osteo II software. Data are expressed as mean \pm SEM per mm^2 . Images were taken with an Olympus BX61 DSU Fluorescent spinning disc confocal microscope and digital camera at the Georgetown

Lombardi Cancer Center Histopathology/Tissue Core Laboratory.

Laboratory analyses

Urine samples were collected for 24 h biweekly by placing the rats into metabolic cages (650–0100, Nalgene) for urine $[\text{Na}^+]$ and osmolality. Survival blood samples (2 ml) were collected by tail vein venipuncture after the first month and nonsurvival blood samples were collected at the end of experiment by right atrial cardiac puncture, both collected under inhalation anesthesia (as described for DXA). Serum and urine $[\text{Na}^+]$ concentrations were measured with a sodium analyzer (Coulter ELISE; Beckman, Fullerton, CA) and osmolality values with a freezing point osmometer (Model 3900; Advanced Instruments, Inc., Norwood, MA). Serum 25OHD and 1,25(OH) $_2$ D, intact PTH, osteocalcin, total and free testosterone, LH, FSH and IGF-1 were measured by immunoassays as described previously (Verbalis et al. 2010). Serum calcium, phosphorus, creatinine, alkaline phosphatase, and albumin were measured via an autoanalyzer (AniLytics).

Statistical analysis

Data are expressed as mean \pm standard error (SE error bars). Multiple groups were compared using ANOVA and Holmes–Sidak tests, and *t*-tests were used for comparing two groups. Statistical significance level was considered at $p < 0.05$.

Results

Serum sodium and osmolality

The protocol described in the “Methods” section produced the expected chronic hyponatremia in the experimental group and maintained normonatremia in the control group. Baseline urine sodium and osmolality were similar in both groups ($p = \text{NS}$). Regular monitoring of urine osmolality confirmed a sustained antidiuresis induced by the desmopressin infusions. Table 1 summarizes the serum and urine indicators of sodium and water homeostasis during the two phases of the study; the differences between the two groups were highly significant for every parameter ($p < 0.001$).

Table 1 Serum and urinary parameters of sodium and water homeostasis

	Normonatremic Phase I	Normonatremic Phase II	Hyponatremic Phase I	Hyponatremic Phase II
Serum [Na ⁺] (mmol/l)	142.7±1.1	139.0±0.3	112.7±1.3*	113.8±2.9 ^a
Serum osmolality (mOsm/kg H ₂ O)		302±2		236±3 ^a
Urine [Na ⁺] excretion (μmol/h)	27.9±5.3	38.3±2.8	56.2±2.2*	78.1±5.6 ^a

* $p < 0.001$ compared to Phase I normonatremic group values

^a $p < 0.001$ compared to Phase II normonatremic group values

Body weight and fat content changes

Rats were adapted to liquid diet for 14 days prior to the induction of hyponatremia. Consistent with previous studies, the process of adaptation to low sodium correlated with liquid diet intake. Daily monitoring of liquid diet intake indicated a 50% reduction within 24 h, followed by gradual increase after 5 days and complete normalization by 10 days. There was no difference between the hyponatremic and normonatremic groups in baseline body weight (BW). The BW in the normonatremic group slightly and gradually increased from the baseline of 499±12 g to a final BW of 536±13 g ($p < 0.05$) on solid diet, whereas BW remained stable in the hyponatremic group on liquid diet (initial BW 504±8 g and final BW 499±11 g; $p = 0.38$). Terminal serum IGF-1 levels, a marker of nutritional status, were normal in both hyponatremic and normonatremic rats, although levels were somewhat higher in the normonatremic group than in the hyponatremic group (1,697±46 vs. 1,431±31 ng/ml; $p < 0.01$). DXA measurements of body composition in the normonatremic group indicated a 6% increase of body fat content from 28.0±0.4% to 35.0±0.8% ($p < 0.001$), of which subcutaneous fat mass increased by 7.1±12.8% and visceral fat mass increased by 22.9±5.8% during the 18-week period. In contrast, total body fat content in the hyponatremic group decreased from 29.0±0.5% to 26.1±0.7% during Phase I ($p < 0.01$), of which subcutaneous fat decreased by 14.8±5.6% and visceral fat decreased by 2.9±7.4%. Body fat content normalized to 29.4±1.1% in the hyponatremic group during Phase II ($p = 0.38$ compared to baseline).

Bone loss: bone mineral density and bone mineral content changes

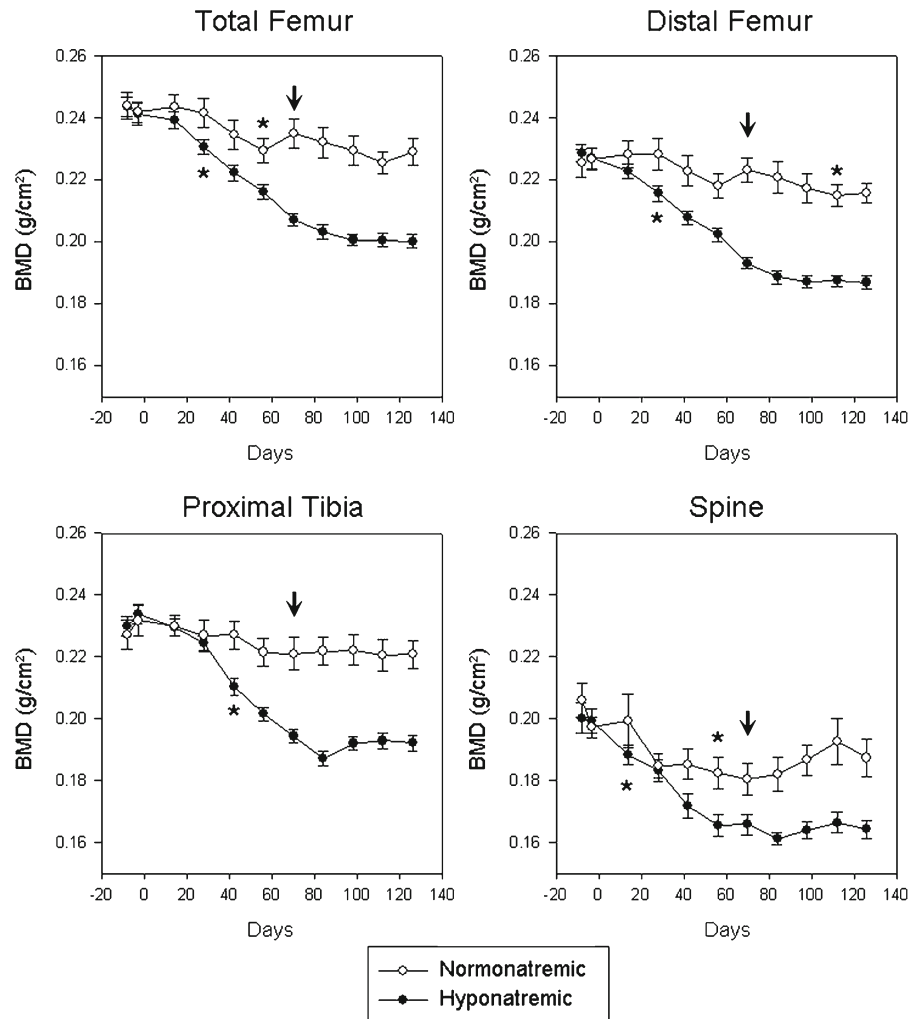
Two baseline measurements showed no significant difference in BMD between the two groups at any

location (L1–L4 vertebrae, $p = 0.643$; total femur, $p = 0.909$; distal femur, $p = 0.715$; proximal tibia, $p = 0.659$). Thereafter, longitudinal in vivo BMD measurements showed slow decreases of bone mass in normonatremic rats (Fig. 1). This decline of BMD was statistically significant first at the L1–L4 vertebrae and at the total femora by 56 days ($p < 0.05$ for both), and at the distal femora by 112 days ($p < 0.01$) compared to baseline values (Fig. 1, asterisks). There was no significant decrease of BMD in normonatremic rats at the proximal tibia compared to baseline (Fig. 1).

Hyponatremic rats lost BMD at a much faster rate than normonatremic rats during Phase I of the study (Fig. 1) The first significant decrease of BMD (indicated by asterisks) at the L1–L4 vertebrae was recorded by 14 days ($p < 0.05$), at the total femora ($p < 0.01$) and distal femora ($p < 0.01$) by 28 days, and at the proximal tibia ($p < 0.05$) by 36 days; BMD decreased progressively in all areas thereafter. Compared to the normonatremic rats, the hyponatremic rats had significantly lower BMD by 14 days at the PA spine ($p < 0.05$), by 28 days at the total femur ($p < 0.05$) and by 42 days at the proximal tibia ($p < 0.01$) (Fig. 1, asterisks). The magnitude of BMD decrease by the end of the Phase I study indicated that bone loss in hyponatremic rats was twice the loss of BMD in normonatremic rats at the L1–L4 vertebrae, 5-fold at the total femora, 12-fold at the distal femora, and 4-fold at the proximal tibiae (Fig. 2). The progressive bone loss was halted when increased vitamin D treatment was introduced to hyponatremic rats during Phase II (Fig. 1, arrows). The differences between the normonatremic and hyponatremic bones did not increase further during Phase II at any of the sites (Fig. 2).

Results of excised bone BMD measurements with DXA confirmed results from in vivo measurements. BMD recorded from excised left femora of rats at the end of Phase II were lower (0.1343±0.0025 g/cm²)

Fig. 1 Longitudinal *in vivo* DXA measurements in aged F344BN rats show bone mineral density (BMD) changes over 18 weeks at multiple sites. Slight losses of BMD in normonatremic rats were as expected for this ageing phenotype. Chronic hyponatremia induced marked and progressive decreases of BMD that significantly exceeded the decrease in the normonatremic rats. Asterisks indicate first statistically significant change of BMD from baseline. Arrows indicate start of vitamin D injections. All data are means \pm SEM



than BMD recorded from excised left femora of normonatremic rats (0.1556 ± 0.0020 g/cm²) ($p < 0.001$).

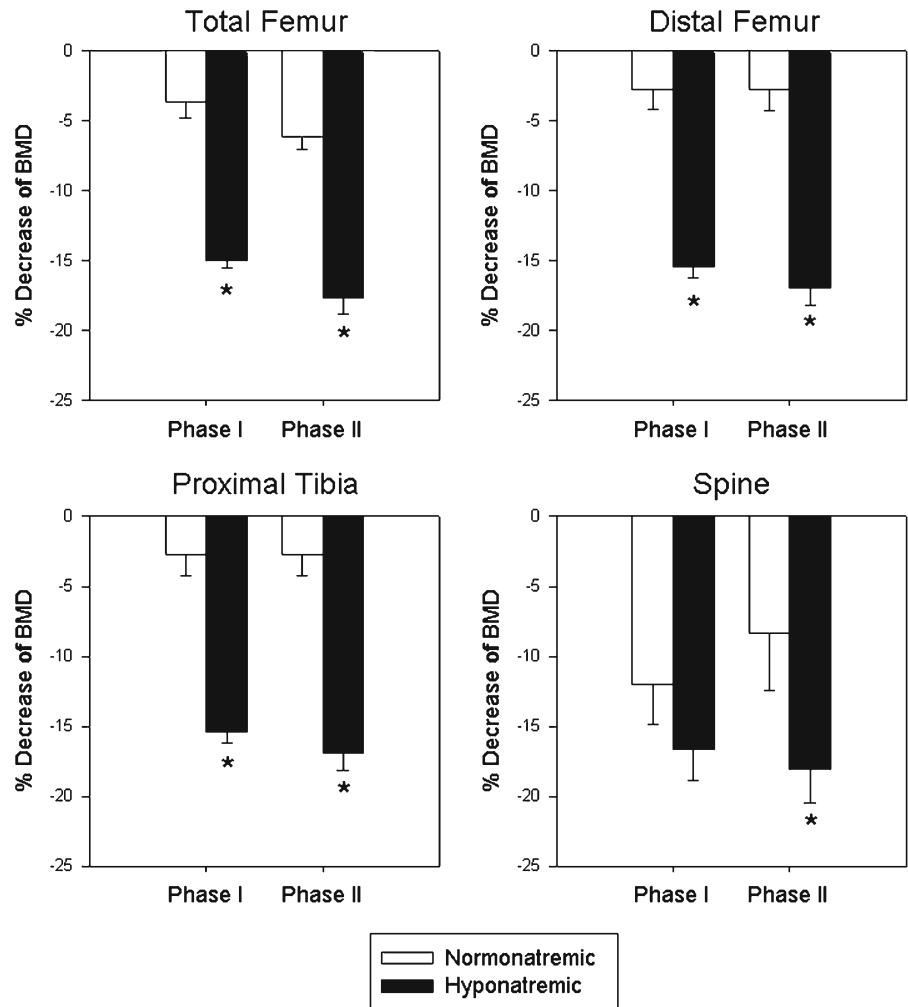
Bone ash analyses confirmed our findings with DXA measurements regarding the difference between hyponatremic and normonatremic BMC at two sites: L1–L2 vertebrae and tibia (Table 2). It is well established that the calcium and phosphorus concentrations of dissolved ash reflect calcium hydroxyl-apatite concentration of bones. Sodium, which is a trace element stored in bone, can also be measured in dissolved ashes. The reduced ash calcium and phosphorus mass in both tibia and L1–L2 vertebrae from hyponatremic rats compared to ash calcium and phosphorus mass in normonatremic rats indicated that bones from the hyponatremic rats had reduced BMC. Notably, the ash sodium mass was significantly reduced by 16.4% in L1–L2 vertebrae and by 8.7% in the tibia from

hyponatremic rats compared to ash sodium in normonatremic rats ($p < 0.05$) (Table 2).

Parameters of calcium metabolism

As shown in Fig. 3, following 10 weeks of hyponatremia (Phase I), serum calcium levels were lower in hyponatremic than in normonatremic rats ($p < 0.001$), and serum phosphorus levels were also slightly, but not significantly, lower (hyponatremic, 4.5 ± 0.3 ; normonatremic, 5.5 ± 0.7 mg/dl; $p = 0.17$). This indicated that the hyponatremic rats may have developed vitamin D deficiency, similarly to the young hyponatremic rats in our previously reported experiments, even though they received double the amounts of vitamin D in their diet compared to the prior studies and compared to the normonatremic rats (Verbalis et al. 2010). This notion

Fig. 2 Changes of bone mineral density (BMD) at multiple sites at the end of Phase I (10 weeks) and Phase II (18 weeks) in normonatremic (*open bars*) and hyponatremic (*black bars*) aged F344BN rats. The rate of BMD decreases from baseline were significantly faster in the hyponatremic rats than in the normonatremic rats ($p < 0.001$). During Phase II, hyponatremic rats received high dose vitamin D supplement that mitigated further declines of BMD. Asterisks indicate statistically significant differences from the normonatremic controls. All data are means \pm SEM



was supported by results of serum 25OHD measurements, the generally accepted indicator of vitamin D status. Despite doubling the vitamin D intake in hyponatremic rats compared to the intake in normonatremic

rats during the first 10 weeks (144 vs. 75 IU/day), serum 25OHD levels were still lower in the hyponatremic group (13.5 ± 0.5 ng/ml) compared to the normonatremic group (45.6 ± 8.5 ; $p < 0.001$) (Fig. 3), although

Table 2 Bone ash analyses in bones from hyponatremic rats

	L1–L2 vertebrae		Tibia	
	Normonatremic	Hyponatremic	Normonatremic	Hyponatremic
Wet weight (g)	1.9980 \pm 0.1609	1.6638 \pm 0.0513**	1.1730 \pm 0.0273	1.1684 \pm 0.0366**
Dry weight (g)	0.8178 \pm 0.0986	0.7462 \pm 0.0266	0.766667 \pm 0.019437	0.7284 \pm 0.01926
Ash weight (mg/bone)	307.8 \pm 27.8	270.0 \pm 16.2	401.1 \pm 10.9	375.4 \pm 9.0*
Calcium mass (mg)	121.78 \pm 7.4	113.38 \pm 10.06*	169.56 \pm 6.9	156.00 \pm 3.3*
Sodium mass (mg)	22.2 \pm 0.56	19.07 \pm 1.54**	19.11 \pm 0.53	15.52 \pm 0.18**

* $p < 0.05$ compared to normonatremic group values

** $p < 0.01$ compared to normonatremic group values

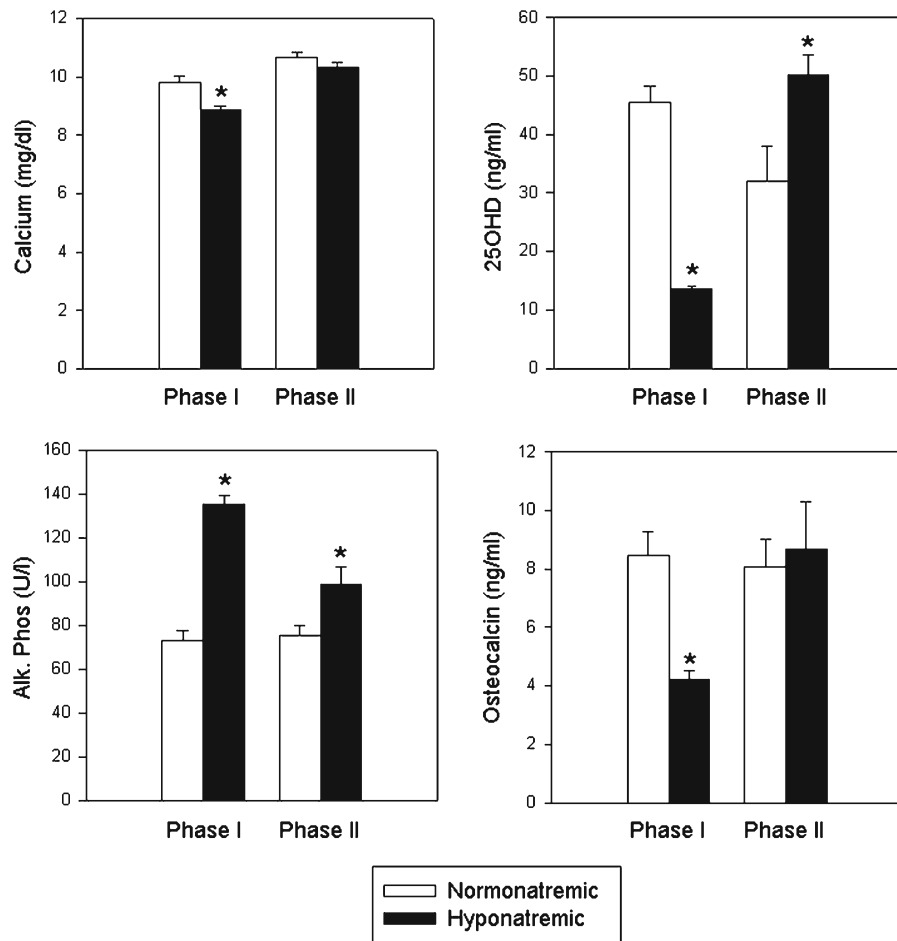


Fig. 3 Parameters of calcium metabolism. Graphs show serum calcium, 25-hydroxy- vitamin D (25OHD), alkaline phosphatase (bone turnover marker) and osteocalcin (bone formation marker) values in normonatremic (open bars) and hyponatremic (black bars) aged F344BN rats at the end of Phase I and Phase II of the study. Results indicate that chronic hyponatremia reduced serum calcium and 25OHD levels, and that a 10-fold increased vitamin D supplementation during Phase II was needed to normalize calcium and 25OHD levels. Serum alkaline phosphatase concentrations

were increased regardless of vitamin D status in the hyponatremic rats compared to the normonatremic rats, consistent with persistently increased bone resorption to liberate sodium from the bone matrix. Reduced osteocalcin in Phase I indicated decreased bone formation, which returned to the levels of the normonatremic rats following vitamin D supplementation in Phase II. Asterisks indicate statistically significant differences from normonatremic controls ($p < 0.05$). All data are means \pm SEM

both values were within normal ranges for rats (10–80 ng/ml). Accordingly, serum PTH concentrations were higher in hyponatremic rats (205.7 ± 41.4 pg/ml) than in the normonatremic rats (77.0 ± 11.0 pg/ml; $p < 0.05$) (normal range 12–80 pg/ml for isoflurane anesthetized rats) (not shown).

Vitamin D is well known to increase osteoblast functions, including osteocalcin secretion from osteoblasts, in rats as well as humans. As shown in Fig. 3, osteocalcin serum levels were significantly reduced in hyponatremic rats compared to normonatremic rats by

the end of Phase I ($p < 0.001$), consistent with reduced vitamin D levels in the hyponatremic rats. To evaluate the impact of vitamin D deficiency, during the Phase II of our study, we supplemented hyponatremic rats with a 10-fold excess vitamin D for 8 weeks. As shown in Fig. 3, this treatment increased 25OHD concentrations in hyponatremic rats above the concentrations in normonatremic rats ($p < 0.05$), and equalized serum calcium ($p = 0.24$) concentrations by increasing values in hyponatremic rats to the levels found in normonatremic rats, both at the end of Phase I and Phase II (Fig. 3). There was

no significant difference in serum $1,25(\text{OH})_2$ Vitamin D_3 concentrations between hyponatremic (17.8 ± 3.1 pg/ml) and normonatremic (19.6 ± 6.4 pg/ml) groups ($p=0.79$) at the end of Phase II (not shown). Osteocalcin concentrations in the hyponatremic group increased by the end of Phase II to equal the concentrations in the normonatremic group ($p=0.79$) (Fig. 3), indicating that the high dose vitamin D supplementation increased bone formation.

The increased bone turnover in hyponatremic rats was indicated by elevated bone-specific alkaline phosphatase concentrations during Phase I ($p<0.001$), which did not normalize by additional vitamin D supplements during Phase II ($p<0.5$), suggesting that increased turnover occurred independently of vitamin D status (Fig. 3).

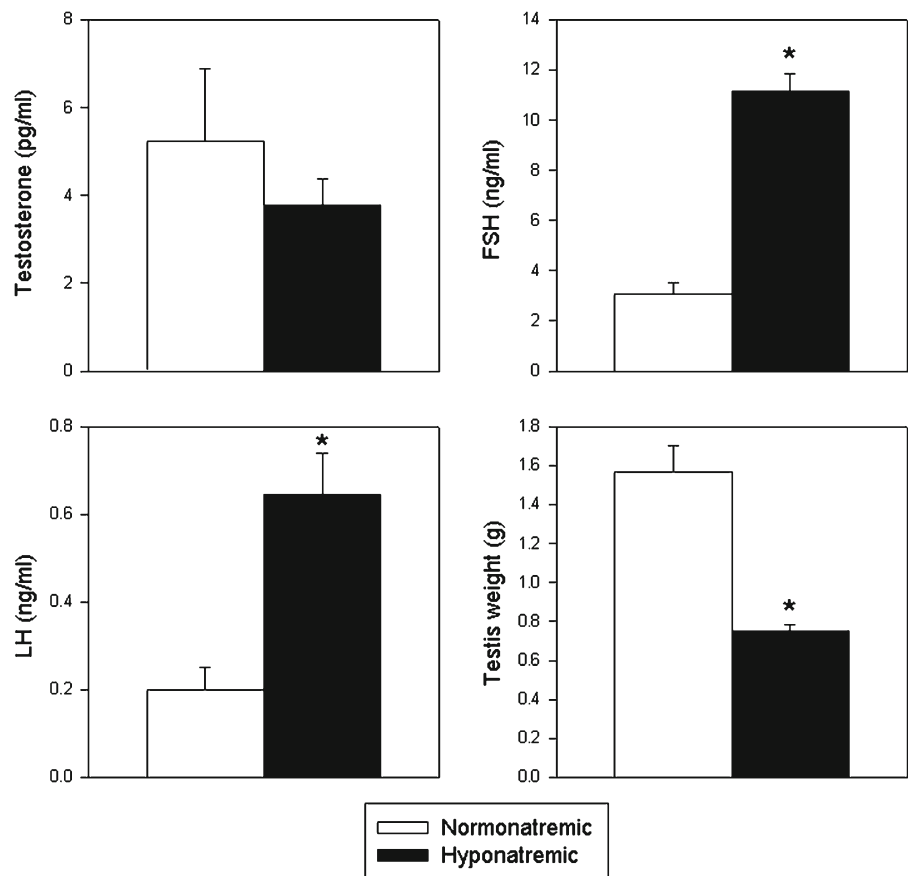
Hypogonadism and impaired spermatogenesis

Testicular weights were markedly lower at autopsy in hyponatremic than in normonatremic rats (Fig. 4). A similar reduction of testes weight was seen in our

previous study of young rats (Verbalis et al. 2010). Analyses of serum samples for free testosterone, FSH and LH indicated that after 10 weeks of hyponatremia (Phase I), hyponatremic rats developed mild hypogonadism (Fig. 4). Serum free testosterone concentrations were minimally, but not significantly, decreased at 3.8 ± 0.6 vs. 5.2 ± 1.7 pg/ml (normal range 0.5–15 ng/ml; $p=0.35$), LH was increased to 0.64 ± 0.09 vs. 0.20 ± 0.05 ng/ml (normal range 0.15–0.70 ng/ml; $p<0.01$), and FSH was increased to 11.18 ± 0.67 vs. 3.05 ± 0.45 ng/ml (normal range 5.6–20 ng/ml; $p<0.001$) in hyponatremic rats compared to normonatremic rats (Fig. 4).

Histological examination indicated that hyponatremia severely impaired spermatogenesis and caused testicular atrophy in hyponatremic rats (Fig. 5). In sections from hyponatremic rats, the size of the seminiferous tubules was markedly reduced, as demonstrated by representative photomicrographs and morphometric analysis (Fig. 5). The images show that the germinal

Fig. 4 Serum-free testosterone and gonadotropin concentrations and testicular weight in normonatremic (open bars) and hyponatremic (black bars) aged F344BN rats at the conclusion of the study. Graphs show that hyponatremic rats had slightly reduced free testosterone (NS) and increased FSH and LH concentrations compared to normonatremic rats. Hypogonadism was also indicated by reduced testes weights at autopsy. Asterisks indicate statistically significant differences from the normonatremic controls ($p<0.001$). All data are means \pm SEM



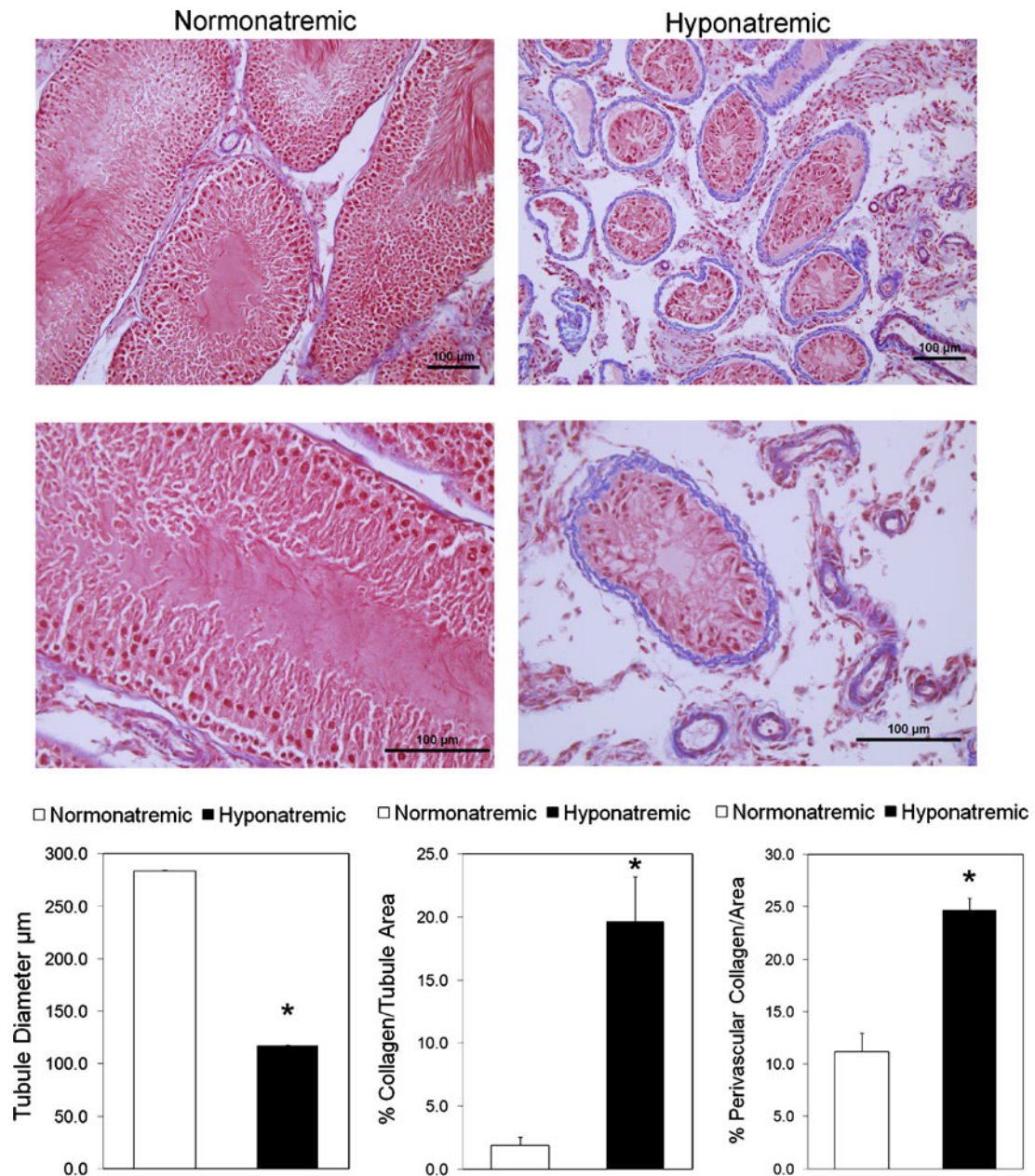


Fig. 5 Histological appearance and morphometric analysis of testes sections from aged F344BN normonatremic and hyponatremic rats. Representative low-power ($\times 20$; upper panels) and high power ($\times 40$; lower panels) microscopic images of 5- μm sections stained with Masson's trichrome protocol that marks collagen fibers with blue color. Images from normonatremic rat testes sections (left panel) show an intact spermatogenesis from the basal layer of spermatogonia, large primary spermatocytes and spermatids in a columnar pattern, and a thin collagen layer surrounding blood vessels and in the lamina propria around the seminiferous tubules. In contrast, images from hyponatremic rat testes sections (right panels) demonstrate markedly reduced size of the seminiferous tubules with severely

impaired spermatogenesis, disorganized basal layer, lack of columnar structure, absence of mature spermatozoa, necrosis and hyalinization in the center, and a thicker layer of collagen surrounding blood vessels and in the lamina propria of the seminiferous tubules. Bars, 100 μm . The graphs show results of morphometric analyses of images from normonatremic (open bar) and hyponatremic (black bars) rat testes, as described in the "Methods" section. The results indicate significant differences in seminiferous tubule size and peritubular and perivascular collagen deposits between the normonatremic and hyponatremic groups. Asterisks indicate statistically significant differences from normonatremic controls ($p < 0.001$). All data are means \pm SEM

epithelium was disorganized and spermatogenesis was arrested in most tubules in micrographs from hyponatremic rat testes. When present, germ cells were detached at different stages of maturation, and the most severely damaged tubules showed complete atrophy with hyalinization. Analysis of Masson's trichrome stained sections from hyponatremic rats revealed striking fibrous degeneration of the lamina propria, as indicated by the peritubular collagen deposits (Fig. 5, photomicrographs and morphometric analysis). In addition, there was also a significant increase in perivascular fibrosis in the hyponatremic group. There was a decrease in the interstitial tissue in sections from hyponatremic rats (Fig. 5), but Leydig cells were still present, though smaller than in the normonatremic rats (not shown). This may explain why the serum testosterone concentrations were only moderately decreased in the hyponatremic rats.

Skeletal sarcopenia

Longitudinal lean mass measurements by DXA analysis encompassed the entire thigh muscle. There was no difference in muscle mass between groups at the beginning of the experiment ($p=0.11$). Results showed a marginal decrease of thigh muscle mass in normonatremic rats over 18 weeks (initial, 16.92 ± 0.31 g; final, 16.5 ± 0.22 g; $p=0.2$), but body composition analysis indicated a small but significant 7% decrease in muscle mass ($p<0.001$) (Fig. 6). In contrast, there was a more pronounced progressive decline of muscle mass in the hyponatremic rats during Phase I of the study, with an initial $3.7\pm 1.0\%$ decrease over the first 2 weeks of hyponatremia ($p<0.01$), followed by a steady decline at a rate of 2.1% per month to a maximum decline of 17% by the end of Phase I (from 16.62 ± 0.16 to 13.68 ± 0.25 g; $p<0.001$ compared to baseline) (Fig. 6). Equalization of vitamin D status by additional high dose vitamin D administration during the Phase II prevented additional declines in lean mass (final, 14.85 ± 0.26 g; $p=0.06$ compared to lean mass at the end of Phase I). There was a statistically significant difference in thigh muscle mass between the normonatremic and hyponatremic groups by the end of Phase I, which remained significantly reduced by the end of Phase II (Fig. 6).

Cardiac hypertrophy and fibrosis

Heart weights, even after adjustment for BW, were markedly increased in hyponatremic rats compared to normonatremic rats ($p<0.01$) (Table 3). To gain insight into the pathogenesis of this heart enlargement, we carried out histomorphometric analyses of sections from the left and right ventricles. Analysis of H&E-stained sections showed reduction of cardiac myocyte number in the hyponatremic group ($p<0.01$), but no difference in cardiac myocyte diameter ($p=0.43$) (Table 3), findings consistent with loss of cardiac myocyte number due to decreased cell division. Histology (Fig. 7) and morphometric analyses (Table 3) indicated a marked increase of collagenous fibrotic material both perivascularly ($p<0.01$) and interstitially ($p<0.001$). This suggests that cardiac fibrosis may represent a component of the increase in heart weight in the hyponatremic rats.

Discussion

This study demonstrated that chronic hyponatremia causes morphological changes in multiple organ systems over an 18-week period of study in aged F344BN rats. Specifically, chronic hyponatremia in this rodent model of aging was found to accelerate and exacerbate multiple pathologies traditionally associated with aging, including bone loss, hypogonadism, reduced adiposity, sarcopenia, and cardiomyopathy.

Previous studies using this protocol have established that maximal hyponatremia develops in 3–5 days after the start of desmopressin infusion in rats fed a liquid diet, and remains stable thereafter for the remainder of the study (Verbalis and Drutarosky 1988; Verbalis et al. 2010). Our earlier studies using this rat model of SIADH demonstrated that chronic lowering the extracellular sodium concentration induces severe loss of BMC in young, growing rats. The current results now extend these findings to old rats, which is of more clinical relevance to the human disease of SIADH. Our data demonstrate that chronic hyponatremia induced progressive bone loss in aged rats. The difference in excised femora BMD between normonatremic and hyponatremic old F344BN rats was 16%, whereas the difference in excised femora BMD in young Sprague–Dawley rats was 30%; however, the younger rats had a 40% higher BMD in the normonatremic group.

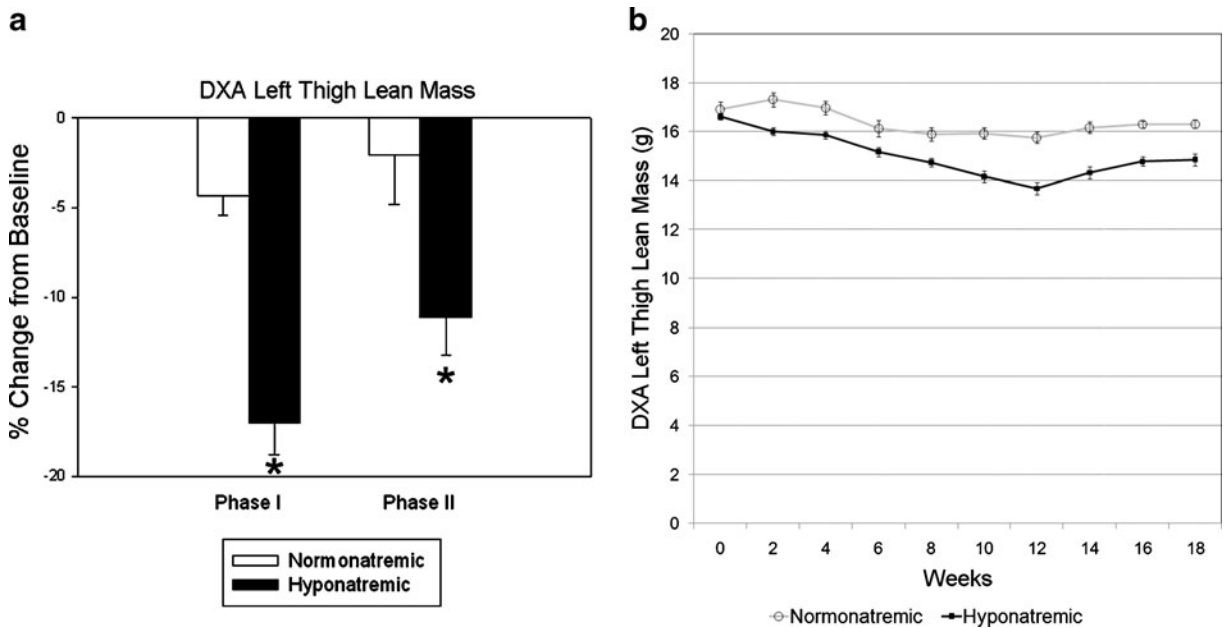


Fig. 6 DXA measurements of thigh muscle mass in normonatremic and hyponatremic aged F344BN rats. On the left, values show percent changes of muscle mass measured in grams from the same region of interest from the beginning of the study (baseline) to the end of Phase I and Phase II of the study in normonatremic (open bars) and hyponatremic (black bars) rats. On the right, longitudinal in vivo DXA lean mass values are

depicted in normonatremic (open label and gray line) and hyponatremic (closed label and black line) rats over the 18 weeks of study. The results indicate that hyponatremia induced marked sarcopenia that was mitigated by the normalization of vitamin D status during Phase II. Asterisks indicate statistically significant differences from normonatremic controls ($p < 0.01$). All data are means \pm SEM

Importantly, longitudinal measurements at multiple sites in older rats that are no longer growing now directly showed a progressive gradual bone loss in the hyponatremic rats, whereas our prior experiment on young growing rats did not include in vivo DXA data. Comparing bone loss at multiple sites (Fig. 1) demonstrated that chronic hyponatremia reduced BMD significantly at the spine 2 weeks earlier than at the limbs. Our findings of the slow decrease of BMD in the control

rats is consistent with a previous report that showed decline of bone mass by ash content between 22 and 28 months of age in F344BN rats (LaMothe et al. 2003).

Bone ash analysis confirmed the findings found using bone densitometry, and additionally provided evidence for changes in mineral composition. Although sodium is a trace element in bone matrix, significant quantities of sodium can be liberated by bone resorption. Our analysis of ash mineral content

Table 3 Increased heart weight, loss of cardiac myocytes, and cardiac fibrosis in hyponatremic rats

	Normonatremic	Hyponatremic
Heart weight/body weight (g/kg)	3.03 \pm 0.19	3.93 \pm 0.37**
No. of myocyte nuclei/mm ² ventricle	6514.04 \pm 308.1	5088.96 \pm 281.6**
Cardiac myocyte diameter (μ m)	14.76 \pm 1.05	15.05 \pm 1.85 ^{NS}
Perivascular collagen area (% of ventricular area)	7.5 \pm 1.9	13.1 \pm 4.5**
Interstitial collagen area (% of ventricular area)	6.1 \pm 0.8	13.1 \pm 2.6***

^{NS} not statistically significant from normonatremic group values

** $p < 0.01$ compared to normonatremic group values

*** $p < 0.001$ compared to normonatremic group values

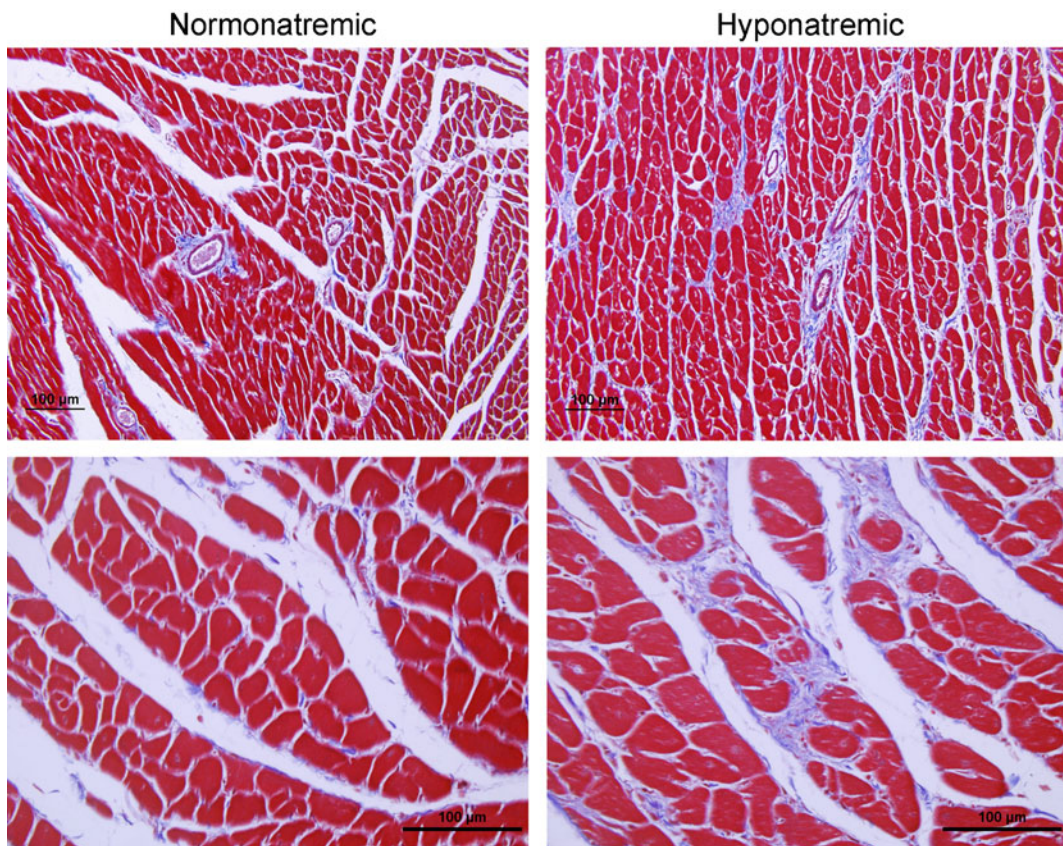


Fig. 7 Histology and morphometric measurements of hearts from normonatremic and hyponatremic aged F344BN rats. Representative low-power ($\times 20$ objective; *upper panels*) and high power ($\times 40$ objective; *lower panels*) microscopic images of 5- μm sections from the hearts stained with Masson's trichrome

protocol that marks collagen fibers with *blue color*. Note increased interstitial and perivascular collagen deposits in micrographs of the left ventricle from hyponatremic rats (*right panels*) compared to micrographs from normonatremic rats (*left panels*). Bars, 100 μm

demonstrated for the first time that chronic hyponatremia reduces sodium content of the tibia and the lumbar vertebrae proportionally to the reduction in calcium content (Table 2). However, this resorbed sodium would not be expected to increase the serum $[\text{Na}^+]$, as it is subsequently lost by urinary excretion as a result of the extracellular fluid volume expansion that is a cardinal feature of SIADH (Schwartz et al. 1957).

The clinical significance of the bone findings in rats was supported by cross-sectional analysis of data from the Third National Health and Nutrition Examination Survey (NHANES III). Among NHANES III participants ≥ 50 years, a statistically significant positive linear association between serum $[\text{Na}^+]$ and femoral neck BMD was detected in the hyponatremic subjects ($p < 0.01$) but not in the normonatremic subjects ($p = 0.99$). After adjusting for multiple potential confounding factors (age, race, sex, BMD, smoking, history of diuretic

use, physical activity), the results showed that among ambulatory participants with hyponatremia the odds for osteoporosis at the hip (BMD T -scores below -2.5) were significantly higher by 2.87-fold (95% CI, 1.41–5.81; $p = 0.003$) compared to those with normonatremia. This almost 3-fold increase of osteoporosis risk in an already vulnerable population for fracture emphasizes the public health importance of understanding the impact of chronic hyponatremia. Consistent with this possibility, two clinical studies have now confirmed a significantly increased incidence of hyponatremia in patients with both outpatient (Gankam et al. 2008) and inpatient (Sandhu et al. 2009) fractures, and more recently two additional longitudinal studies independently demonstrated that even mild hyponatremia increases fracture incidence (Kinsella et al. 2010; Hoorn et al. 2011).

This hyponatremia-induced bone loss is largely due to increased bone resorption, as demonstrated by our

previous histomorphometric analysis of bones from young rats that indicated 7-fold increased osteoclast counts associated with the trabecular surfaces of bones from hyponatremic rats compared to normonatremic rats (Verbalis et al. 2010). Moreover, our previous studies on osteoclast cultures demonstrated a direct effect of low extracellular $[\text{Na}^+]$ to activate osteoclastogenesis and osteoclastic bone resorption in both RAW264.7 derived and bone marrow-derived cultures (Barsony et al. 2010).

In addition to increased bone resorption, our prior studies also indicated reduced bone formation in hyponatremic rats, indicating an uncoupling of bone resorption and bone formation. Dynamic histomorphometry using double calcein labeling indicated nearly 50% reduction of the mineral apposition rate and bone formation rate per bone surface, both of which are bone formation parameters, in sections from hyponatremic rats compared with normonatremic rats. Serum osteocalcin was lower in young hyponatremic rats in our prior experiments (Verbalis et al. 2010), and was similarly reduced in old rats in this experiment. By administering 10-fold increased vitamin D during Phase II of this study, we increased bone formation as evidenced by normalization of serum osteocalcin. This intervention in hyponatremic rats halted the progressive bone loss despite ongoing accelerated bone resorption, presumably by restoring the coupling of bone resorption and bone formation. In vitro studies aimed at understanding the mechanisms of decreased osteoblast activity and increased osteoclast activation found a sodium concentration-dependent decrease in the activity of the sodium-dependent ascorbic acid transporter, and a resulting decrease in ascorbic acid uptake into RAW264.7 murine pre-osteoclastic cells (Barsony et al. 2010) and into MCT3T-E1 murine osteoblast-like cells (unpublished results). Ascorbic acid is essential for osteoblast functions, including osteocalcin secretion (Wu et al. 2003), and is a negative regulator of osteoclastogenesis (Xiao et al. 2005). The decreased intracellular ascorbic acid concentration weakened the defense against oxidative stress, increased the accumulation of free reactive oxygen radicals, and elicited oxidative stress response from these cells (Barsony et al. 2010). The active form of vitamin D has been reported to protect against oxidative stress in multiple tissues (Jung et al. 2011), in addition to its more established roles to stimulate osteoblastic bone formation and mineralization (Nakane et al. 2006). Future prospective clinical studies will be required to

elucidate whether patients with chronic hyponatremia would benefit from increased vitamin D intake, in addition to antiresorptive treatments.

In addition to the direct effect of low extracellular sodium on osteoclastogenesis and increased bone resorption, mild hypogonadism may also contribute to the observed bone loss in males. Our previous findings in young hyponatremic male rats showed more severe hypogonadism compared to normonatremic controls than the hypogonadism in aged rats presented here. Aging itself caused hypogonadism in the normonatremic rats in this study, thereby decreasing the differences between the hyponatremic and normonatremic aged rats. In both studies, the observed hypogonadism was accompanied by marked hyponatremia-induced testicular atrophy. This testicular atrophy and arrest of spermatogenesis could also be related to impaired ascorbic acid uptake as a result of low extracellular sodium concentrations. Consistent with this potential mechanism, a similar impairment of spermatogenesis has been reported in mice unable to synthesize ascorbic acid (Yazama et al. 2006). Other factors may also be involved. Elegant recent studies have indicated connections between bone and testes (Ferron et al. 2011; Oury et al. 2011), and between osteoporosis and sarcopenia (Bhasin 2003; Frisoli et al. 2010). Using cell culture studies and cell-specific loss- and gain-of-function models, Karsenty's team demonstrated that the bone-derived hormone osteocalcin regulates male fertility, signals through a G protein-coupled receptor, *Gprc6a*, in Leydig cells to regulate testosterone production, and promotes spermatogenesis and germ cell survival (Oury et al. 2011). Gonadal functions are well-established regulators of skeletal muscle and bone health, and now even more evidence points to a cross-talk between the skeleton, muscle, and energy metabolism. In another study, this group reported that injections of uncarboxylated osteocalcin increased insulin secretion from pancreatic β -cells, improved insulin sensitivity, and prevented high fat diet-induced type 2 diabetes in mice. Mice treated with intermittent osteocalcin injections had additional mitochondria in their skeletal muscle, had increased energy expenditure, and were protected from diet-induced obesity. Interestingly, the ablation of osteoblasts in adult mice not only confirmed a role of osteocalcin in glucose metabolism, but also indicated that other osteoblast-derived hormones may contribute to the emerging function of the skeleton as a regulator of energy metabolism (Yoshikawa et al. 2011). Studies of mice with osteoblast-

specific ablation of insulin receptor completed the feed-forward loop. Mice lacking insulin receptor in osteoblasts had low circulating under-carboxylated osteocalcin and reduced bone acquisition due to decreased bone formation and deficient numbers of osteoblasts (Fulzele et al. 2010). Further studies using this rat model of hyponatremia may elucidate the roles of reduced osteocalcin in the pathogenesis of the testicular and muscle deterioration observed in these studies.

This study also provides initial evidence for the induction by chronic hyponatremia of multiple manifestations of frailty beyond osteoporosis. Loss of appetite and subcutaneous fat is a well recognized feature of senile frailty. Unlike normonatremic aged rats that still gained weight and increased adiposity between 22 and 27 months of age, as previously reported for male F344BN rats (Carter et al. 2010; LaMothe et al. 2003), hyponatremic rats maintained weight but lost both subcutaneous and visceral adiposity even though serum IGF-1 levels did not decrease sufficiently to indicate undernutrition (i.e., below 800 ng/ml for male rats) (Bourrin et al. 2000). Similar age-related adiposity loss in normonatremic F344 × BN rats was not observed until after 36 months of age (LaMothe et al. 2003), suggesting that the age-related fat loss was accelerated by the hyponatremic state.

Progressive loss of skeletal muscle mass, or sarcopenia, is also a well recognized feature of senile frailty, and also occurs in the F344BN rat model of aging (Baker and Hepple 2006; Paturi et al. 2010). The normonatremic aged rats had a modest decline in lean mass, whereas the hyponatremic rats experienced a pronounced progressive 17% decrease in thigh muscle mass over this period, which was ameliorated but not reversed by vitamin D treatment. Similar to the adiposity results, this suggests that the age-related sarcopenia was accelerated by the hyponatremic state. Both the loss of adipose and muscle mass occurred relative to normonatremic rats that were fed quantities of isocaloric diet that maintained equivalent BWs in both groups during the course of the study. Potential contributing factors to hyponatremia-induced reduction of appendicular skeletal mass in our rat model include hypogonadism, vitamin D deficiency (Rolland et al. 2011), and possibly decreased mobility. Although chronically hyponatremic rats exhibit grossly normal activity patterns by observation, more subtle degrees of decreased motor activity may occur during nocturnal periods and contribute to the observed decreases in

both muscle mass and bone. In humans, sarcopenia affects 25% of those aged over 80 years, and has been shown to predict increased falls and fracture risk, creating the phenotype recently termed “sarco-osteoporosis” (Buehring et al. 2010). Our results suggest that chronic hyponatremia should be added to the conditions identified to cause sarcopenia and increased fall risk in the elderly (Fielding et al. 2011).

Age-related cardiomyopathy with ventricular hypertrophy and fibrosis has been reported in rodent models and in humans, and has been associated with increased oxidative stress (Kakarla et al. 2010). Increased collagen content and myocardial fibrosis was detected in old rodents (Boyle et al. 2011; Bradshaw et al. 2010; Hacker et al. 2006; Lin et al. 2008). Our results demonstrated both of these findings in the hyponatremic F344BN aged rats compared to the normonatremic aged rats. It is striking that the significantly increased heart weight in the hyponatremic rats was accompanied by a decreased density of myocyte nuclei, indicating decreased myocyte numbers, and only slight increases in measured myocyte diameter. This suggests that the major contributory factor to the increased heart weight was not cardiac hypertrophy, but rather a combination of increased heart water content and fibrosis. In this regard, the long-standing strong association between hyponatremia and adverse outcomes in heart failure patients (Lee et al. 2003; Packer et al. 1987) has never been adequately explained. Our results suggest that chronic hyponatremic may exacerbate the cardiac remodeling process known to occur in congestive heart failure, which leads to progressive cardiac dysfunction and death.

Senescence-associated chronic disorders have been described extensively, and include senile osteoporosis characterized by low bone mass and fragility (Manolagas 2010), sarcopenia (Almeida et al. 2007; Frisoli et al. 2010), cardiac fibrosis (Wang et al. 2010), and hypogonadism (Sampson et al. 2007). Our results show effects of chronic hyponatremia to induce or exacerbate all of these processes. These findings suggest the possibility that hyponatremia can aggravate multiple manifestations of senescence, and may therefore represent an independent risk factor for the development and progression of age-associated infirmities. Although the mechanisms for each of these effects remain to be ascertained, the findings are consistent with our cellular studies indicating that lowering extracellular sodium concentration

increases the expression of biomarkers of oxidative stress both in vivo and in vitro (Barsony et al. 2010). Reduced defenses against cellular damage caused by reactive oxygen species as a result of the hyponatremic state represents a viable hypothesis for the effects seen in multiple organ systems of the hyponatremic F344BN rats, and suggests that hyponatremia may act via this, and associated pathways, to accelerate the aging process. This could explain long-standing clinical findings that hyponatremia is an independent risk factor for increased mortality in multiple diseases (Wald et al. 2010), including hospitalized elderly patients (Terzian et al. 1994). Future prospective studies in patients with SIADH may indicate whether correction of serum sodium can diminish multiple age-related comorbidities in this population.

In summary, this study provides initial evidence for multiple adverse consequences of chronic hyponatremia beyond gait abnormalities and increased fracture risks. Loss of adiposity, sarcopenia, and cardiomyopathy will need to be explored in more detail in this rodent model of SIADH, and perhaps in other models of hyponatremia. Additional studies will be needed to gain mechanistic insight into the hyponatremia-induced sarcopenia and cardiomyopathy, including detailed analysis of the signaling mechanisms in organ and cell culture models. Also important will be future studies aimed at exploring the prevention or reversibility of these hyponatremia-induced changes following correction of hyponatremia in rats, and eventually clinical studies in humans using vasopressin receptor antagonists. The ultimate goal of this and future derivative studies is understanding of how chronic hyponatremia impacts on the long-term health of the large number of elderly individuals with this common metabolic disorder.

Acknowledgements This study was supported by grant R01-AG029477 from the National Institute on Aging. The authors are grateful for imaging technical help to Eva CA Permaul.

References

- Almeida M, Han L, Martin-Millan M, Plotkin LI, Stewart SA, Roberson PK, Kousteni S, O'Brien CA, Bellido T, Parfitt AM, Weinstein RS, Jilka RL, Manolagas SC (2007) Skeletal involution by age-associated oxidative stress and its acceleration by loss of sex steroids. *J Biol Chem* 282:27285–27297
- Baker DJ, Hepple RT (2006) Elevated caspase and AIF gene expression correlate with progression of sarcopenia during aging in male F344BN rats. *Exp Gerontol* 41:1149–1156
- Barsony J, Sugimura Y, Verbalis JG (2010) Osteoclast response to low extracellular sodium and the mechanism of hyponatremia-induced bone loss. *J Biol Chem* 286(12):10864–10875
- Bergstrom WH, Wallace WM (1954) Bone as a sodium and potassium reservoir. *J Clin Invest* 33:867–873
- Bhasin S (2003) Testosterone supplementation for aging-associated sarcopenia. *J Gerontol A Biol Sci Med Sci* 58:1002–1008
- Boscoe A, Paramore C, Verbalis JG (2006) Cost of illness of hyponatremia in the United States. *Cost Eff Resour Alloc* 4:10
- Bourrin S, Toromanoff A, Ammann P, Bonjour JP, Rizzoli R (2000) Dietary protein deficiency induces osteoporosis in aged male rats. *J Bone Miner Res* 15:1555–1563
- Boyle AJ, Shih H, Hwang J, Ye J, Lee B, Zhang Y, Kwon D, Jun K, Zheng D, Sievers R, Angeli F, Yeghiazarians Y, Lee R (2011) Cardiomyopathy of aging in the mammalian heart is characterized by myocardial hypertrophy, fibrosis and a predisposition towards cardiomyocyte apoptosis and autophagy. *Exp Gerontol* 46:549–559
- Bradshaw AD, Baicu CF, Rentz TJ, Van Laer AO, Bonnema DD, Zile MR (2010) Age-dependent alterations in fibrillar collagen content and myocardial diastolic function: role of SPARC in post-synthetic procollagen processing. *Am J Physiol Heart Circ Physiol* 298:H614–H622
- Buehring B, Krueger D, Binkley N (2010) Jumping mechanography: a potential tool for sarcopenia evaluation in older individuals. *J Clin Densitom* 13:283–291
- Buford TW, Anton SD, Judge AR, Marzetti E, Wohlgenuth SE, Carter CS, Leeuwenburgh C, Pahor M, Manini TM (2010) Models of accelerated sarcopenia: critical pieces for solving the puzzle of age-related muscle atrophy. *Ageing Res Rev* 9:369–383
- Capasso JM, Palackal T, Olivetti G, Anversa P (1990) Severe myocardial dysfunction induced by ventricular remodeling in aging rat hearts. *Am J Physiol* 259:H1086–H1096
- Carter CS, Giovannini S, Seo DO, Dupree J, Morgan D, Chung HY, Lees H, Daniels M, Hubbard GB, Lee S, Ikeno Y, Foster TC, Buford TW, Marzetti E (2010) Differential effects of enalapril and losartan on body composition and indices of muscle quality in aged male Fischer 344 × Brown Norway rats. *Age (Dordr)* 33(2):167–183
- Ferron M, McKee MD, Levine RL, Ducy P, Karsenty G (2011) Intermittent injections of osteocalcin improve glucose metabolism and prevent type 2 diabetes in mice. doi:10.1016/j.bone.2011.04.017
- Fielding RA, Vellas B, Evans WJ, Bhasin S, Morley JE, Newman AB, van Abellan KG, Andrieu S, Bauer J, Breuille D, Cederholm T, Chandler J, De MC, Donini L, Harris T, Kannt A, Keime GF, Onder G, Papanicolaou D, Rolland Y, Rooks D, Sieber C, Souhami E, Verlaan S, Zamboni M (2011) Sarcopenia: an undiagnosed condition in older adults. Current consensus definition: prevalence, etiology, and consequences. International working group on sarcopenia. *J Am Med Dir Assoc* 12:249–256
- Frisoli A Jr, Chaves PH, Ingham SJ, Fried LP (2010) Severe osteopenia and osteoporosis, sarcopenia, and frailty status in community-dwelling older women: Results from the Women's Health and Aging Study (WHAS) II. *Bone* 48(4):952–957

- Fulzele K, Riddle RC, DiGirolamo DJ, Cao X, Wan C, Chen D, Faugere MC, Aja S, Hussain MA, Bruning JC, Clemens TL (2010) Insulin receptor signaling in osteoblasts regulates postnatal bone acquisition and body composition. *Cell* 142:309–319
- Gankam KF, Andres C, Sattar L, Melot C, Decaux G (2008) Mild hyponatremia and risk of fracture in the ambulatory elderly. *Q J Med* 101:583–588
- Greenberg A, Verbalis JG (2006) Vasopressin receptor antagonists. *Kidney Int* 189(12):2124–2130
- Hacker TA, McKiernan SH, Douglas PS, Wanagat J, Aiken JM (2006) Age-related changes in cardiac structure and function in Fischer 344 × Brown Norway hybrid rats. *Am J Physiol Heart Circ Physiol* 290:H304–H311
- Hawkins RC (2003) Age and gender as risk factors for hyponatremia and hypernatremia. *Clin Chim Acta* 337:169–172
- Hoom EJ, Rivadeneira F, van Meurs JB, Ziere G, Stricker BH, Hofman A, Pols HA, Zietse R, Uitterlinden AG, Zillikens MC (2011) Mild hyponatremia as a risk factor for fractures: The Rotterdam Study. *J Bone Miner Res* 26(8):1822–1828
- Jung EM, Choi KC, Jeung EB (2011) Expression of calbindin-D28k is inversely correlated with proapoptotic gene expression in hydrogen peroxide-induced cell death in endometrial cancer cells. *Int J Oncol* 38:1059–1066
- Kakarla SK, Fannin JC, Keshavarzian S, Katta A, Paturi S, Nalabotu SK, Wu M, Rice KM, Manzoor K, Walker EM Jr, Blough ER (2010) Chronic acetaminophen attenuates age-associated increases in cardiac ROS and apoptosis in the Fischer Brown Norway rat. *Basic Res Cardiol* 105:535–544
- Kinsella S, Moran S, Sullivan MO, Molloy MG, Eustace JA (2010) Hyponatremia independent of osteoporosis is associated with fracture occurrence. *Clin J Am Soc Nephrol* 5:275–280
- LaMothe JM, Hepple RT, Zernicke RF (2003) Selected contribution: bone adaptation with aging and long-term caloric restriction in Fischer 344 × Brown-Norway F1-hybrid rats. *J Appl Physiol* 95:1739–1745
- Lee DS, Austin PC, Rouleau JL, Liu PP, Naimark D, Tu JV (2003) Predicting mortality among patients hospitalized for heart failure: derivation and validation of a clinical model. *JAMA* 290:2581–2587
- Lin J, Lopez EF, Jin Y, Van RH, Bauch T, Han HC, Lindsey ML (2008) Age-related cardiac muscle sarcopenia: Combining experimental and mathematical modeling to identify mechanisms. *Exp Gerontol* 43:296–306
- Manolagas SC (2010) From estrogen-centric to aging and oxidative stress: a revised perspective of the Pathogenesis of osteoporosis. *Endocr Rev* 31(3):266–300
- Manolagas SC, Parfitt AM (2010) What old means to bone. *Trends Endocrinol Metab* 21:369–374
- Miyazaki T, Ohmoto K, Hirose T, Fujiki H (2010) Chronic hyponatremia impairs memory in rats: effects of vasopressin antagonist tolvaptan. *J Endocrinol* 206:105–111
- Nakane M, Fey TA, Dixon DB, Ma J, Brune ME, Li YC, Wu-Wong JR (2006) Differential effects of Vitamin D analogs on bone formation and resorption. *J Steroid Biochem Mol Biol* 98:72–77
- Oury F, Sumara G, Sumara O, Ferron M, Chang H, Smith CE, Hermo L, Suarez S, Roth BL, Ducy P, Karsenty G (2011) Endocrine regulation of male fertility by the skeleton. *Cell* 144:796–809
- Packer M, Lee WH, Kessler PD, Gottlieb SS, Bernstein JL, Kukin ML (1987) Role of neurohormonal mechanisms in determining survival in patients with severe chronic heart failure. *Circulation* 75:IV80–IV92
- Paturi S, Gutta AK, Katta A, Kakarla SK, Arvapalli RK, Gadde MK, Nalabotu SK, Rice KM, Wu M, Blough E (2010) Effects of aging and gender on muscle mass and regulation of Akt-mTOR-p70s6k related signaling in the F344BN rat model. *Mech Ageing Dev* 131:202–209
- Perrien DS, Akel NS, Dupont-Versteegden EE, Skinner RA, Siegel ER, Suva LJ, Gaddy D (2007) Aging alters the skeletal response to disuse in the rat. *Am J Physiol Regul Integr Comp Physiol* 292:R988–R996
- Renneboog B, Musch W, Vandemergel X, Manto MU, Decaux G (2006) Mild chronic hyponatremia is associated with falls, unsteadiness, and attention deficits. *Am J Med* 119:71–78
- Rolland Y, Dupuy C, van KG Abellan, Gillette S, Vellas B (2011) Treatment strategies for sarcopenia and frailty. *Med Clin North Am* 95:427–438, ix
- Sampson N, Untergasser G, Plas E, Berger P (2007) The ageing male reproductive tract. *J Pathol* 211:206–218
- Sandhu HS, Gilles E, DeVita MV, Panagopoulos G, Michelis MF (2009) Hyponatremia associated with large-bone fracture in elderly patients. *Int Urol Nephrol* 41:733–737
- Schwartz WB, Bennett W, Curelop S, Bartter FC (1957) A syndrome of renal sodium loss and hyponatremia probably resulting from inappropriate secretion of antidiuretic hormone. *Am J Med* 23:529–542
- Simon MR (1984) The rat as an animal model for the study of senile idiopathic osteoporosis. *Acta Anat (Basel)* 119:248–250
- Sohal RS, Weindruch R (1996) Oxidative stress, caloric restriction, and aging. *Science* 273:59–63
- Swynghedauw B, Besse S, Assayag P, Carre F, Chevalier B, Charlemagne D, Delcayre C, Hardouin S, Heymes C, Moalic JM (1995) Molecular and cellular biology of the senescent hypertrophied and failing heart. *Am J Cardiol* 76:2D–7D
- Terzian C, Frye EB, Piotrowski ZH (1994) Admission hyponatremia in the elderly: factors influencing prognosis. *J Gen Intern Med* 9:89–91
- Verbalis JG, Barsony J, Sugimura Y, Tian Y, Adams DJ, Carter EA, Resnick HE (2010) Hyponatremia-induced osteoporosis. *J Bone Miner Res* 25:554–563
- Verbalis JG, Drutarosky MD (1988) Adaptation to chronic hypoosmolality in rats. *Kidney Int* 34:351–360
- Wahr PA, Michele DE, Metzger JM (2000) Effects of aging on single cardiac myocyte function in Fischer 344 × Brown Norway rats. *Am J Physiol Heart Circ Physiol* 279:H559–H565
- Wald R, Jaber BL, Price LL, Upadhyay A, Madias NE (2010) Impact of hospital-associated hyponatremia on selected outcomes. *Arch Intern Med* 170:294–302
- Wang C, Leung A, Sinha-Hikim AP (1993) Reproductive aging in the male Brown-Norway rat: a model for the human. *Endocrinology* 133:2773–2781
- Wang M, Zhang J, Walker SJ, Dworakowski R, Lakatta EG, Shah AM (2010) Involvement of NADPH oxidase in age-associated cardiac remodeling. *J Mol Cell Cardiol* 48:765–772
- Wu X, Itoh N, Taniguchi T, Nakanishi T, Tatsu Y, Yumoto N, Tanaka K (2003) Zinc-induced sodium-dependent vitamin C transporter 2 expression: potent roles in osteoblast differentiation. *Arch Biochem Biophys* 420:114–120

Xiao XH, Liao EY, Zhou HD, Dai RC, Yuan LQ, Wu XP (2005) Ascorbic acid inhibits osteoclastogenesis of RAW264.7 cells induced by receptor activated nuclear factor kappaB ligand (RANKL) in vitro. *J Endocrinol Invest* 28:253–260

Yazama F, Furuta K, Fujimoto M, Sonoda T, Shigetomi H, Horiuchi T, Yamada M, Nagao N, Maeda N (2006)

Abnormal spermatogenesis in mice unable to synthesize ascorbic acid. *Anat Sci Int* 81:115–125

Yoshikawa Y, Kode A, Xu L, Mosialou I, Silva BC, Ferron M, Clemens TL, Economides AN, Kousteni S (2011) Genetic evidence points to an osteocalcin-independent influence of osteoblasts on energy metabolism. *J Bone Miner Res* 26(9):2012–2025